



Cite this: *Dalton Trans.*, 2018, **47**, 3669

Received 21st December 2017,

Accepted 24th January 2018

DOI: 10.1039/c7dt04828a

rsc.li/dalton

## Fluorescent antitumor titanium(IV) salen complexes for cell imaging†

Avia Tzuber<sup>a</sup>, Naomi Melamed-Book<sup>b</sup> and Edit Y. Tshuva<sup>id</sup> \*<sup>a</sup>

**Two differently substituted fluorescent salen Ti(IV) complexes were developed. One was inactive on human cancer cells, whereas the other showed high cytotoxicity. Based on live cell imaging, both complexes penetrated the cell, but were not detected in the nuclei. Moreover, the inactive complex was trapped in endocytic vesicles, whereas the active complex accumulated in the perinuclear region and inflicted phototoxicity upon continuous irradiation.**

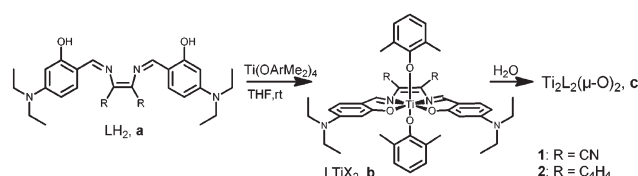
Titanium(IV) complexes are highly attractive candidates for anticancer therapy.<sup>1</sup> After the platinum anticancer compounds, titanium(IV) complexes, in particular titanocene dichloride (Cp<sub>2</sub>TiCl<sub>2</sub>) and budotitan (bzaac)<sub>2</sub>Ti(OEt)<sub>2</sub>, were the first to enter clinical trials<sup>2</sup> due to their high and wide activity *in vitro* and *in vivo*, accompanied by low toxicity, ultimately producing the non-toxic titanium dioxide in aqueous solutions.<sup>1–3</sup> Nevertheless, these Ti(IV) compounds failed clinical trials due to their low hydrolytic stability in biological environment that led to the formation of undefined aggregates with low solubility, which also hampered mechanistic investigations.

Previously, we introduced anticancer Ti(IV) complexes based on phenolato ligands, which presented exceptional hydrolytic stability combined with high cytotoxicity and *in vivo* activity.<sup>1b,c,4</sup> In particular, Ti(IV) LTiX<sub>2</sub> type complexes based on diamino-bis(phenolato) salan and salen ligands with two labile alkoxo groups were investigated, exhibiting activity often greater than that of cisplatin with slow hydrolysis to eventually yield highly stable and defined phenolato polynuclear clusters.<sup>4e,g,5</sup> Despite the different geometries of the salan and salen complexes, similar mechanisms were suggested based on their similar reactivity with a bidentate chelating ligand and similar hydrolytic behavior.<sup>4g</sup> Structure–activity studies indicated strong

impact of the ligand substitution on complex performance: steric bulk decreased activity, and hydrophobicity decreased solubility and accessibility and by that, affected reactivity.<sup>4d,5a,6</sup>

Very little is known about the mechanism of cytotoxicity of Ti(IV) complexes.<sup>1b,c</sup> Specifically, when analyzing potential cellular targets, various studies have been performed with older and newer compounds, the results of which are not all consistent. Although some studies pointed to possible interactions with DNA based on accumulation in nucleic acid-rich areas and various adducts identified, others suggested alternative mechanisms involving, for instance, enzyme inhibition.<sup>1c</sup> Herein, we utilize the photophysical features of the planar highly-conjugated salen system for the detection of Ti(IV) complexes in living cells using confocal fluorescence microscopy to shed light on the cellular bio-distribution of the cytotoxic phenolato Ti(IV) complexes. The  $\pi$ -conjugated system of the bis-Schiff base salen ligands can be modulated by particular substitutions on the amine bridge and/or the phenolato rings to enhance fluorescence.<sup>7</sup> Such salen chelating ligands were previously used as optical probes for cations such as Cu(II), Pt(II), Al(III), and Zn(II),<sup>8</sup> and salen Zn(II) complexes were employed as fluorescent markers for cell imaging.<sup>9</sup>

To enhance intramolecular charge transfer, diethylamino-substituted phenolato rings were employed, and two complexes were synthesized with cyano-substituted or phenylene-diamine bridges (Scheme 1). The ligands **1a** and **2a** were prepared according to a known procedure *via* a condensation reaction between substituted salicylaldehyde and the conjugated diamine.<sup>7a</sup> The Ti(IV) complexes **1b** and **2b** were prepared as previously discussed for related compounds by reacting **1a** and



**Scheme 1** Fluorescent Ti(IV) salen complexes investigated.

<sup>a</sup>Institute of Chemistry, The Hebrew University of Jerusalem, Jerusalem 9190401, Israel. E-mail: edit.tshuva@mail.huji.ac.il

<sup>b</sup>The Bio-Imaging Unit, The Alexander Silberman Institute of Life Sciences, The Hebrew University of Jerusalem, Jerusalem 9190401, Israel

† Electronic supplementary information (ESI) available: Details of experimental procedures, spectroscopic data and crystal data of **2b**. CCDC 1584442. For ESI and crystallographic data in CIF or other electronic format see DOI: 10.1039/c7dt04828a



**2a**, respectively, with one equiv. of titanium tetrakis(dimethylphenoxide) to obtain the Ti(IV) complexes in high yields.<sup>4f,g</sup> <sup>1</sup>H and <sup>13</sup>C NMR analyses of the products confirmed the formation of a single isomer with high symmetry due to the single set of signals for the phenolato moiety of the salen ligand and a single type of a labile ligand. Single crystals of **1b** and **2b** were obtained from diethyl ether and dichloromethane, respectively, at −35 °C. Although the structure of **1b** was of low quality (Fig. S1†), Fig. 1 depicts the ORTEP drawing of **2b** along with selected bond lengths and angles.† Both structures clearly feature mononuclear octahedral *C*<sub>2v</sub>-symmetrical complexes with *trans* binding of the two labile dimethylphenoxo ligands. Furthermore, the bond lengths and angles of **2b** around the metal center are similar to those of related Ti(IV) salen complexes.<sup>4f,g</sup>

The cytotoxicity of **1b** and **2b** was evaluated on human colon HT-29 and cervix HeLa cancer cell lines using the methylthiazolyldiphenyl-tetrazolium (MTT) assay to establish cell viability (Fig. 2).<sup>10</sup> Complex **2b** exhibited high antitumor

activity with IC<sub>50</sub> values ranging from 3.3 to 9.3 μM, which are among the lowest values obtained for this family.<sup>4f,g</sup> In contrast, **1b** was inactive toward both cell lines tested. It was suspected that the electron withdrawing cyano groups in **1b** reduce the stability or affect cellular penetration due to reduced lipophilicity. The free salen ligand **2a** analyzed as the control showed significantly lower reactivity (Fig. S7†).

The comparative hydrolytic stability of **1b** and **2b** was evaluated upon the addition of 10% D<sub>2</sub>O (*ca.* 1000 equiv. relative to Ti) to *d*<sub>6</sub>-DMSO solutions of the complexes, as previously described for related Ti(IV) compounds (Fig. S2†).<sup>4d,g,11</sup> Spectra were collected every few minutes and the integration of selected signals of the labile 2,6-dimethylphenoxo ligands was measured relative to an internal standard. The hydrolytic stability of both complexes was similar with the *t*<sub>1/2</sub> values for the labile ligand hydrolysis of 50 and 20 minutes for **1b** and **2b** respectively, ruling out reduced hydrolytic stability as the reason for the inactivity of **1b**. Throughout the hydrolysis, single polynuclear species were separately obtained for each complex with no indication of salen ligand release even after 3 days. These products featured high symmetry, which indicated formation of either the di- or the tetra-nuclear product, as reported recently for related complexes,<sup>4g,11</sup> whereby MS analysis supported the specific formation of a dimeric structure as characteristic for the salen family of complexes (Fig. S3†).<sup>4g</sup> The spectra of the hydrolysis products did not change even upon the addition of 10 000 H<sub>2</sub>O equivalents to the parent complexes and stirring for 3 days, confirming the formation of a single defined cluster (Fig. S2c†).

The hydrolytic behaviour of the complexes implied that the active species derived from **2b** is its defined hydrolysis product.<sup>4e,12</sup> Thus, to evaluate the possible reactivity of both hydrolysis products, complexes **1b** and **2b** were separately reacted with 10 000 equivalents of H<sub>2</sub>O and the hydrolysis products **1c** and **2c** (Scheme 1) were isolated (Fig. S4 and S2c†). Their cytotoxicity was measured on HT-29 and HeLa cells, as described above. Although the hydrolysis product **1c** was inactive like its parent complex, **2c** exhibited high cytotoxicity with IC<sub>50</sub> values comparable to those of its monomeric precursor and even better for the HeLa cell line (Fig. 3). Previous reports presented the cytotoxic

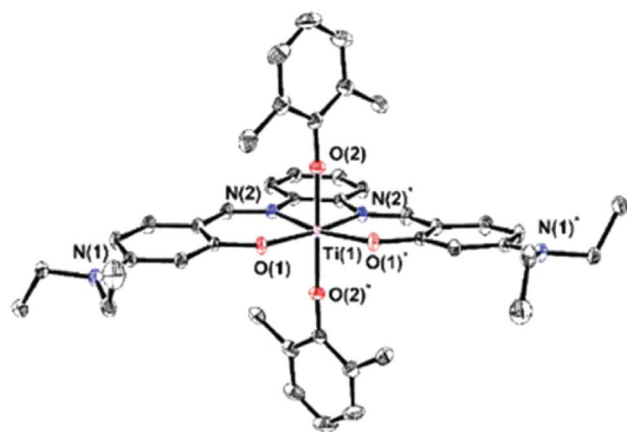


Fig. 1 ORTEP drawing of **2b**† with 50% probability ellipsoids; H atoms and dichloromethane solvent molecule were omitted for clarity. Selected bond lengths [Å] and angles [°]: Ti(1)–N(2) 2.143(2), Ti(1)–O(1) 1.904(2), Ti(1)–O(2) 1.874(2), O(1)–Ti(1)–O(2) 89.17(7), O(1)\*–Ti(1)–O(1) 109.47(7), O(2)\*–Ti(1)–O(2) 177.7(1), N(2)\*–Ti(1)–N(2) 74.9(1), O(2)–Ti(1)–N(2) 90.25(7), and O(1)–Ti(1)–N(2) 87.88(7).

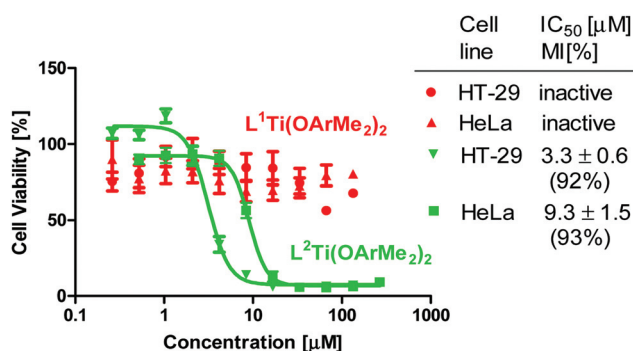


Fig. 2 Dependence of HT-29 and HeLa cell viability (based on MTT assay after 3 days incubation) on concentration of **1b** and **2b**, which is presented on a logarithmic scale.

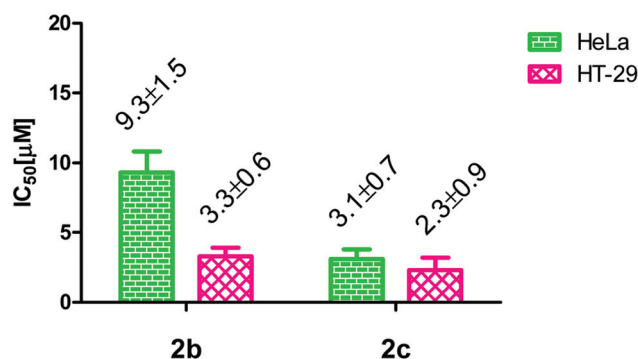


Fig. 3 IC<sub>50</sub> values (μM) of **2b** and **2c** on different cell types: HT-29 and HeLa cells.



activities of such defined polynuclear hydrolysis products based on salan ligands but only in formulations to increase solubility and accessibility<sup>12a</sup> or toward more sensitive murine cancer cell lines.<sup>12b</sup> Thus, this first observation of high activity of a defined phenolato cluster toward a relatively resistant human cancer cell line indicates the enhanced solubility and accessibility of **2c**, and supports the overall conclusion that the hydrolysis product is the active species in the cell.

Studies with fluorescent Ti(IV) complexes are scarce<sup>13</sup> because fluorescence quenching often occurs due to the electron-poor d<sup>0</sup> Ti(IV) metal, which involves strong ligand to metal charge transfer.<sup>13</sup> Nevertheless, **1b** and **2b** are highly emissive in DMSO with red emission for **1b** and green-yellow emission for **2b**, with similar features for their hydrolysis products **1c** and **2c**, respectively (Fig. S5, S6 and Table S1†). Additionally, having two related complexes in hand, one cytotoxic and one inactive, provided an opportunity to compare the two with respect to cellular bio-distribution. Thus, viable cells treated with **1b** and **2b** were evaluated using confocal fluorescence microscopy. The treatment of human cervical HeLa cells separately with 5  $\mu$ M of **1b** and **2b** for only a few minutes resulted in the development of a strong red emission under excitation at 561 nm for **1b** and green emission under excitation at 488 nm for **2b** in the cytoplasm (Fig. 4). Interestingly, despite being inactive, **1b** crossed the cell membrane relatively rapidly and also accumulated in the cytoplasm; therefore, its inactivity apparently does not result from its inability to enter the cell due to insufficient solubility/lipophilicity. Additionally, the defined hydrolysis products **1c** and **2c** were similarly analyzed at a concentration of 2  $\mu$ M, and similar results and accumulation patterns were observed to those obtained for the parent complexes **1b** and **2b**, respectively.

The subcellular accumulation of **1b** and **2b** and **1c** and **2c** was further investigated by staining the organelles with specific fluorescence probes: Hoechst® for staining the nuclei blue and MitoTracker® green or deep red for staining the mitochondria (applied for 1 or 2, respectively). Interestingly, no significant colocalization was detected for the Ti(IV) complexes, and in particular, no indication of entering the nuclei was observed.<sup>13</sup> For the inactive **1b** and its hydrolysis product **1c** the signals appeared as spots and could be mapped as vesicles in the cytoplasm of the treated cells (Fig. 5, lines 1 and 2, respectively). These vesicles spread in the cell cytoplasm and their concentration increased with incubation time. This form

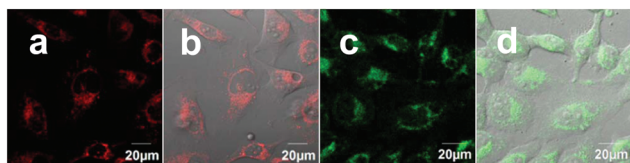


**Fig. 4** Confocal images of the Ti(IV) complexes after incubation in HeLa cells for ca. 5 minutes: (a) **1b** excited at 561 nm; (b) merge image of the fluorescence with DIC image; (c) **2b** excited at 488 nm and (d) merge image of the fluorescence with DIC image.

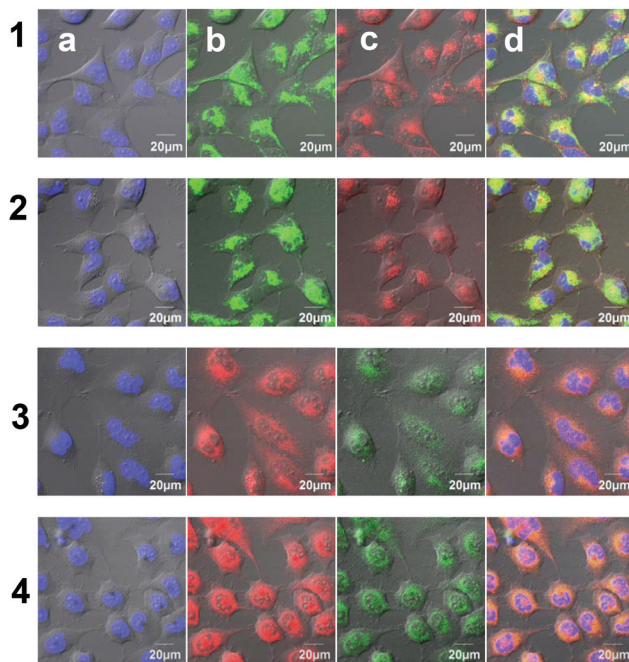


**Fig. 5** Fluorescence colocalization images merged with the DIC image of HeLa cells incubated for 1 hour with **1b** (5  $\mu$ M with 0.2% DMSO in medium, line 1), **1c** (2  $\mu$ M with 0.2% DMSO in medium, line 2), **2b** (5  $\mu$ M with 0.2% DMSO in medium, line 3) and **2c** (2  $\mu$ M with 0.5% DMSO in medium, line 4) and commercial dyes Hoechst® (a) and MitoTracker® (b), Ti(IV) compound (c) and merged images of (a)–(c) (d).

of accumulation suggests that **1b/1c** enter the cells *via* endocytosis in the form of endocytic vesicles and are transported towards the cytoplasm, as observed previously for Ru(II) complexes.<sup>14</sup> Interestingly, a different process was observed for the cytotoxic **2b** and its hydrolysis product **2c**. These complexes crossed the membrane rapidly, possibly by diffusion, and accumulated in the perinuclear region, which could be associated with the endoplasmic reticulum (ER) domain or the Golgi apparatus, as presented in Fig. 5, lines 3 and 4, respectively. Some correlation was observed with MitoTracker®, which may result from mitochondria swelling. Thus, treatment with cytotoxic Ti(IV) compounds could induce mitochondrial dysfunction which eventually leads to apoptotic cell death. Interestingly, a previous study with Pt(II) complexes also showed accumulation in the ER region and induction of ER-stress and cell apoptosis,<sup>15</sup> unlike the common observations of the nuclei as the target of Pt(II) complexes.<sup>16</sup> Notably, the free ligand **2a**, which was analyzed as the control, accumulated differently as defined spots near the nuclei (Fig. S8†).

Following the addition of 5  $\mu$ M of **2b** to HeLa cells, as described above, and incubation under continuous irradiation (every 5–7 minutes), the viable cell population dramatically decreased, much more rapidly than expected (Fig. 6). After only 3 hours the cells underwent cell death and displayed cell shrinkage, loss of cell contact, and membrane blebbing (Fig. 2c, line 6), which are characteristic of early apoptosis.<sup>17</sup> Despite the high cytotoxicity of **2b**, such rapid cell death is not





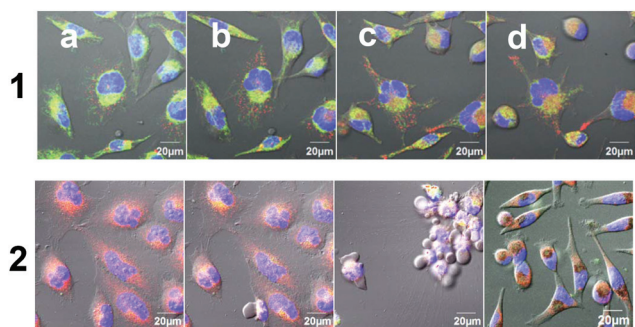


**Fig. 6** Merged fluorescence colocalization images with the DIC image of HeLa cells incubated with **1b** for 1 (a), 4 (b), 9 (c) and 16 (d) hours with continuous irradiation (5  $\mu$ M with 0.5% DMSO in medium, line 1) and **2b** for 1 (a), 2 (b) and 3 (c) hours with continuous irradiation and image of overnight incubation with no continuous irradiation (d) (5  $\mu$ M with 0.2% DMSO in medium, line 2) all with commercial dyes; blue for Hoechst®, green or red for MitoTracker® and red or green for the Ti(IV) complex.

expected under the mild conditions employed. Interestingly, when different areas in the cell plate that did not undergo irradiation were measured, the majority of cells remained viable as expected (Fig. 6, line 2d). In contrast, for the inactive **1b**, no indication of enhanced cell death was detected under irradiation, even after 16 hours of incubation under these conditions (Fig. 6, line 1). Thus, it is obvious that irradiation speeds up cell death, but only for the cytotoxic compound with a markedly lower effect for the control ligand **2a** (Fig. S9†). Such phototoxicity was also observed for a cytotoxic Pt(II) complex of the salen ligand **2a** (**2a-Pt**: Scheme S1 and Fig. S10†), which was analyzed as the control, showing accelerated cell death upon irradiation presumably due to its characteristic electronic properties.<sup>15</sup>

To conclude, we introduced herein the first fluorescent cytotoxic Ti(IV) complexes based on salen ligands bound directly to the metal that can be detected in live cells by confocal fluorescence microscopy. The cell imaging methodology offered new explanations for the factors limiting activity, which could not have been deduced based on the *in vitro* studies alone. Both the active and inactive complexes crossed the cell membrane and penetrated rapidly into the cytoplasm, which demonstrated that cell penetration is not a limiting factor for any of the compounds tested, despite their different lipophilicities. Nevertheless, the differently substituted inactive **1b** seemed to accumulate in vesicles, which could have prevented its cytotoxicity by disabling its access to the biological target, possibly leading to decomposition in the lysosomes as the last stage of the endocytic pathway. In contrast, unlike the mildly active free ligand **2a**, the cytotoxic **2b** and its suggested active species **2c** localized in the perinuclear region. These complexes could also be further light-activated for significantly increased cytotoxic activity due to an associated phototoxicity process, which was also previously encountered with Pt(II) and Ru(II) complexes.<sup>15,18</sup> This provides an additional possible advantage of the salen Ti(IV) complexes for application in controlled anticancer therapy. Further studies

with additional detection techniques are required to unequivocally determine the biological target of these promising anti-cancer Ti(IV) complexes.

## Conflicts of interest

There are no conflicts to declare.

## Acknowledgements

We thank Dr B Bogoslavsky for X-ray analysis. Funding was received from the European Research Council (ERC) under the European Union's Horizon 2020 research and innovation programme (grant agreement 681243).

## Notes and references

- (a) E. Meléndez, *Crit. Rev. Oncol. Hematol.*, 2002, **42**, 309; (b) S. A. Loza-Rosas, M. Saxena, Y. Delgado, K. Gaur, M. Pandrala and A. D. Tinoco, *Metallomics*, 2017, **9**, 346; (c) M. Cini, T. D. Bradshaw and S. Woodward, *Chem. Soc. Rev.*, 2017, **46**, 1040; (d) E. Y. Tshuva and M. Miller, in *Metallo-Drugs: Development and Action of Anticancer Agents*, Walter de Gruyter, Berlin, 2018, vol. 18, pp. 219–249; (e) K. M. Buettner and A. M. Valentine, *Chem. Rev.*, 2012, **112**, 1863; (f) W. A. Wani, S. Prashar, S. Shreaz and S. Gomez-Ruiz, *Coord. Chem. Rev.*, 2016, **312**, 67.
- (a) P. Köpf-Maier and H. Köpf, *Chem. Rev.*, 1987, **87**, 1137; (b) G. Lümme, H. Sperling, H. Luboldt, T. Otto and H. Rubben, *CANCER Chemother. Pharmacol.*, 1998, **42**, 415; (c) T. Schilling, K. B. Keppler, M. E. Heim, G. Niebch, H. Dietzfelbinger, J. Rastetter and A. R. Hanauske, *Invest. New Drugs*, 1995, **13**, 327; (d) B. K. Keppler, C. Friesen, H. G. Moritz, H. Vongerichten and E. Vogel, *Struct. Bonding*, 1991, **78**, 97; (e) F. Caruso, M. Rossi and C. Pettinari, *Expert Opin. Ther. Pat.*, 2001, **11**, 969; (f) N. Kröger, U. R. Kleeberg, K. Mross, L. Edler and D. K. Hossfeld, *Oncol. Res. Treat.*, 2000, **23**, 60.
- (a) F. Caruso, L. Massa, A. Gindulyte, C. Pettinari, F. Marchetti, R. Pettinari, M. Ricciutelli, J. Costamagna, J. C. Canales, J. Tanski and M. Rossi, *Eur. J. Inorg. Chem.*, 2003, 3221; (b) I. Kostova, *Anticancer Agents Med. Chem.*, 2009, **9**, 827; (c) K. Strohsfeldt and M. Tacke, *Chem. Soc. Rev.*, 2008, **37**, 1174; (d) J. H. Toney and T. J. Marks, *J. Am. Chem. Soc.*, 1985, **107**, 947; (e) P. Köpf-Maier and H. Köpf, *Struct. Bonding*, 1988, **70**, 103; (f) A. Sigel and H. Sigel, *Metal complexes in tumor diagnosis and as anticancer agents*, Marcel Dekker, Inc., New York, 2004; (g) F. Caruso and M. Rossi, *Mini-Rev. Med. Chem.*, 2004, **4**, 49.
- (a) M. Shavit, D. Peri, C. M. Manna, J. S. Alexander and E. Y. Tshuva, *J. Am. Chem. Soc.*, 2007, **129**, 12098; (b) E. Y. Tshuva and D. Peri, *Coord. Chem. Rev.*, 2009, **253**, 2098; (c) E. Y. Tshuva and J. A. Ashenhurst, *Eur. J. Inorg. Chem.*, 2009, 2203; (d) D. Peri, S. Meker, M. Shavit and



- E. Y. Tshuva, *Chem. – Eur. J.*, 2009, **15**, 2403; (e) D. Peri, S. Meker, C. M. Manna and E. Y. Tshuva, *Inorg. Chem.*, 2011, **50**, 1030; (f) A. Tzuberly and E. Y. Tshuva, *Inorg. Chem.*, 2011, **50**, 7946; (g) A. Tzuberly and E. Y. Tshuva, *Inorg. Chem.*, 2012, **51**, 1796; (h) M. Miller, O. Braitbard, J. Hochman and E. Y. Tshuva, *J. Inorg. Biochem.*, 2016, **163**, 250.
- 5 (a) T. A. Immel, U. Groth and T. Huhn, *Chem. – Eur. J.*, 2010, **16**, 2775; (b) T. A. Immel, M. Debiak, U. Groth, A. Bürkle and T. Huhn, *ChemMedChem*, 2009, **4**, 738; (c) T. A. Immel, U. Groth, T. Huhn and P. Öhlschläger, *PLoS One*, 2011, **6**, 1.
- 6 (a) H. Glasner and E. Y. Tshuva, *J. Am. Chem. Soc.*, 2011, **133**, 16812; (b) H. Glasner and E. Y. Tshuva, *Inorg. Chem.*, 2014, **53**, 3170; (c) M. Miller and E. Y. Tshuva, *Eur. J. Inorg. Chem.*, 2014, 1485.
- 7 (a) J. Cheng, K. Wei, X. Ma, X. Zhou and H. Xiang, *J. Phys. Chem. C*, 2013, **117**, 16552; (b) C. J. Whiteoak, G. Salassa and A. W. Kleij, *Chem. Soc. Rev.*, 2012, **41**, 622.
- 8 Representative examples: (a) L. Zhou, P. Cai, Y. Feng, J. Cheng, H. Xiang, J. Liu, D. Wu and X. Zhou, *Anal. Chim. Acta*, 2012, **735**, 96; (b) L. Zhou, Y. Feng, J. Cheng, N. Sun, X. Zhou and H. Xiang, *RSC Adv.*, 2012, **2**, 10529; (c) S. Samanta, B. Nath and J. B. Baruah, *Inorg. Chem. Commun.*, 2012, **22**, 98; (d) Y. Zhou, H. N. Kim and J. Yoon, *Bioorg. Med. Chem. Lett.*, 2010, **20**, 125.
- 9 (a) D. Xie, J. Jing, Y.-B. Cai, J. Tang, J.-J. Chen and J.-L. Zhang, *Chem. Sci.*, 2014, **5**, 2318; (b) Y. Hai, J.-J. Chen, P. Zhao, H. Lv, Y. Yu, P. Xu and J.-L. Zhang, *Chem. Commun.*, 2011, **47**, 2435.
- 10 N. Ganot, S. Meker, L. Reyman, A. Tzuberly and E. Y. Tshuva, *J. Visualized Exp.*, 2013, e50767.
- 11 A. Tzuberly and E. Y. Tshuva, *Eur. J. Inorg. Chem.*, 2017, 1695.
- 12 (a) S. Meker, K. Margulis-Goshen, E. Weiss, S. Magdassi and E. Y. Tshuva, *Angew. Chem., Int. Ed.*, 2012, **51**, 10515; (b) S. Meker, K. Margulis-Goshen, E. Weiss, O. Braitbard, J. Hochman, S. Magdassi and E. Y. Tshuva, *ChemMedChem*, 2014, **9**, 1294.
- 13 (a) G. Khalil, C. Orvain, L. Fang, L. Barloy, A. Chaumont, C. Gaiddon, M. Henry, N. Kyritsakas and P. Mobian, *Dalton Trans.*, 2016, **45**, 19072; (b) O. Florès, A. Trommenschlager, S. Amor, F. Marques, F. Silva, L. Gano, F. Denat, M. P. Cabral Campello, C. Goze, E. Bodio and P. Le Gendre, *Dalton Trans.*, 2017, **46**, 14548.
- 14 W.-K. Tsui, L.-H. Chung, M. M.-K. Wong, W.-H. Tsang, H.-S. Lo, Y. Liu, C.-H. Leung, D.-L. Ma, S.-K. Chiu and C.-Y. Wong, *Sci. Rep.*, 2015, **5**, 9070.
- 15 T. Zou, C.-N. Lok, Y. M. E. Fung and C.-M. Che, *Chem. Commun.*, 2013, **49**, 5423.
- 16 (a) J. Gao, Y.-G. Liu and R. A. Zingaro, *Chem. Res. Toxicol.*, 2009, **22**, 1705; (b) N. Kumari, B. K. Maurya, R. K. Koiri, S. K. Trigun, S. Saripella, M. P. Coogan and L. Mishra, *MedChemComm*, 2011, **2**, 1208.
- 17 V. H. S. van Rixel, B. Siewert, S. L. Hopkins, S. H. C. Askes, A. Busemann, M. A. Siegler and S. Bonnet, *Chem. Sci.*, 2016, **7**, 4922.
- 18 J. Hess, H. Huang, A. Kaiser, V. Pierroz, O. Blacque, H. Chao and G. Gasser, *Chem. – Eur. J.*, 2017, **23**, 9888.

